Contents lists available at ScienceDirect

Chemical Engineering Research and Design

journal homepage: www.elsevier.com/locate/cherd

Influence of hydrochloric acid concentration on the demineralization of cortical bone

Margarida Figueiredo[a,*], *Sara Cunha*[a], *Gabriela Martins*[a], *João Freitas*[b], *Fernando Judas*[b], *Helena Figueiredo*[c]

[a] *Chemical Engineering Department, University of Coimbra, Rua Sílvio Lima, 3030-790 Coimbra, Portugal*
[b] *Orthopaedics Department, Coimbra University Hospital (HUC), Praceta Mota Pinto, 3000-075 Coimbra, Portugal*
[c] *Histology Institute, Medicine Faculty, University of Coimbra, Rua Larga, 3004-504 Coimbra, Portugal*

ABSTRACT

Although demineralized bone matrix has been considered a successful grafting material, combining both osteoconductive and osteoinductive properties, conflicting results have been published in the literature regarding its bone-inducing abilities. This may be a consequence of following different demineralization procedures that naturally result in products with different properties.

The present work examines the evaluation of the demineralization process of similar samples of human cortical bone using three different concentrations of hydrochloric acid solutions (0.6 M, 1.2 M and 2.4 M). Sample calcium content was determined (by Atomic Absorption Spectroscopy) at various immersion times, allowing the construction of the corresponding kinetic profiles. Phase and chemical composition were enabled by X-Ray Diffraction Spectroscopy and Fourier Transform Infrared Analysis, respectively. Structural modifications were followed by Light and Scanning Electron Microscopy and quantified by mercury porosimetry (in terms of porosity and pore size distribution).

As expected, increasing the acid concentration led to an increase in the demineralization rate, but not in a proportional way. However, one of the most significant effects of the acid concentration was found on the sample structural features. In fact, a considerable increment in porosity was detected for the sample subjected to the highest hydrochloric acid concentration. Microscopic observations demonstrated that despite the structural deformation resultant from demineralization, the basic microstructure was preserved.

Keywords: Human bone; Demineralization; Kinetics; XRD; FTIR; Porosity

1. Introduction

Demineralized bone matrix (DBM) is often applied in orthopedics, periodontics, oral and maxillofacial surgery because of its inherent osteoconductive and osteoinductive properties (Bauer and Muschler, 2000; Eppley et al., 2005). It can be used either alone (Libin et al., 1975; Morone and Boden, 1998; Pietrzak et al., 2005) or in combination with bone marrow, autogenous bone graft, or other materials (Nade and Burwell, 1977; Kim et al., 2002; Kucukkolbasi et al., 2009). After surface manipulation (namely by chemical modification), demineralized bone has also been found promising as an effective carrier for therapeutic delivery in bone infective sites (Murugan and Ramakrishna, 2004). Additionally, DBM exhibits elastic features, being easily shaped to fill osteochondral lesions with different shapes and sizes (Costa et al., 2001).

Although it is recognized that the process of demineralization exposes proteins, growth factors (specifically the bone morphogenetic proteins (BMPs)) and other bioactive molecules (Urist, 1965; Tuli and Singh, 1978; Katz et al., 2008), the biological bases for the bone-inducing abilities of DBM remain obscure (Colnot et al., 2005). Besides, the demineralization procedure might affect DBM characteristics, yielding to products with distinct biological, chemical and morphological properties. This inevitably leads to distinctive final performances, including osteoinductive potential (Lee et al.,

* *Corresponding author*. Tel.: +351 239798700.
E-mail addresses: mmf@eq.uc.pt (M. Figueiredo), saracunha7@hotmail.com (S. Cunha), agtmartins@gmail.com (G. Martins), jpmarcos@iol.pt (J. Freitas), fernandojudas@gmail.com (F. Judas), mhfigueiredo@fmed.uc.pt (H. Figueiredo).
Received 15 July 2009; Received in revised form 18 March 2010; Accepted 15 April 2010
0263-8762/$ – see front matter © 2010 The Institution of Chemical Engineers. Published by Elsevier B.V. All rights reserved.
doi:10.1016/j.cherd.2010.04.013

2005; Lomas et al., 2001; Peterson et al., 2004; Bae et al., 2006), which can justify the conflicting results found in the literature. In fact, different demineralization protocols have been adopted (Nade and Burwell, 1977; Walsh and Christiansen, 1995; Zhang et al., 1997), using not only different acids (and acid concentrations) but also different grafting materials (cortical or cancelous bone) under distinct configurations (from long bone to blocks and particles with different shape and size characteristics). In addition, donor specifications (Lohmann et al., 2001; Traianedes et al., 2004) and preservation methods (freeze-dried or fresh frozen) (Martin et al., 1999; Schwartz et al., 1996) have also proven to influence the properties of DBM. Furthermore, correlations with morpho-structural changes caused by demineralization are seldom described in the literature.

The process of bone demineralization is normally carried out by immersing the sample in a variety of strong and/or weak acids. In the case of using HCl (the most frequently used acid), the major inorganic constituent of bone (hydroxyapatite) reacts to form monocalcium phosphate and calcium chloride (Horneman et al., 2004; Dorozhkin, 1997). Bone samples are usually demineralized in 0.5–0.6 M HCl in order to remove bone mineral efficiently while leaving the graft osteoinductive (Pietrzak et al., 2009). However, and as mentioned before, sometimes the objective of bone demineralization is just to provide a flexible material regardless of its osteoinductive potential, or an "inert" matrix (containing no significant amount of signal molecule content) to be used in some clinical and research applications.

The kinetics of demineralization has been investigated in samples with planar and cylindrical geometries, confirming that this is a diffusive rate limited process with a sharp advancing reaction front (Lewandrowski et al., 1996, 1997; Hansen, 1974). Special emphasis has been given to the penetration depth of this reaction front throughout the process, including its visual evaluation using SEM (Lewandrowski et al., 1997).

Despite the extensive use of demineralized bone allografts in clinical practice as well as in tissue engineering applications, systematic works regarding their physico-chemical properties are relatively scarce regardless of being reported that these properties play a major role in the final graft performance. The influence of structural elements as porosity and pore size, for instance, is recognized as an important factor to promote cellular migration and adhesion in bone grafts, enhancing its biointegration (Karageorgiou and Kaplan, 2005).

The present study aimed to evaluate the effect of using high concentrations of hydrochloric acid ([HCl] $\geq$ 0.6 M) on the demineralization rate and on the physical and chemical characteristics of similar samples of human cortical bone under block form (as currently used in bone banking procedures). For that purpose, the residual calcium content of the samples was measured (by Atomic Absorption Spectroscopy) as a function of the immersion time, for each acid concentration tested, enabling to evaluate the corresponding kinetic profiles. X-Ray Diffraction and Fourier Transform Infrared Spectroscopy were used to assess phase and chemical alterations. Finally, the influence of acid concentration on structural and morphological features of the specimens was examined by Light and Scanning Electron Microscopy, and quantified by Mercury Intrusion with respect to porosity and pore size distribution.

2. Materials and methods

2.1. Bone samples

The starting material used in this study was a human femur from a 39-year-old male donor, supplied by the bone bank of Coimbra University Hospital (Portugal) (Judas et al., 2005). The femoral diaphysis, with a length about 35 cm and around 4 cm diameter, was transversely cut into 1 cm thickness slices which were afterwards sectioned into four similar pieces. In addition to these samples (1/4 slice), taken as reference in the demineralization studies, some larger specimens (half slices) were reserved for porosity analysis. It should be mentioned that whenever trabecular bone was found inside the diaphysis, it was carefully removed to obtain only compact bone samples.

All samples were degreased through immersion in an alcohol series (ethanol at 70%, v/v), followed by washing with distilled water. They were then kept in hydrogen peroxide (30%, v/v) for at least 48 h and rinsed again. Finally, they were stored in formaldeyde solution (4%, v/v) at 4 °C.

Before use, the samples were thoroughly rinsed with distilled water and subsequently dried in a vacuum oven at 40 °C until constant weight. Samples dry weight (referred to as "initial weight") ranged from 1.6 to 2 g for the standard samples to nearly 4 g for the larger samples (half slices).

Analytical grade type I collagen and hydroxyapatite, purchased from Sigma–Aldrich (Portugal), were used to obtain the corresponding FTIR spectra for comparison with control and demineralized samples.

2.2. Demineralization procedure

The demineralization process started by placing each individual sample over a piece of gauze (to avoid contact with the bottom of the bath) in 200 cm^3 HCl aqueous solution, independently of the samples weight and acid concentration (0.6 M, 1.2 M and 2.4 M). For the lowest acid concentration, this volume is at least four times in excess to that needed to demineralize the sample (21 cm^3 of 0.6 M HCl are needed to demineralize 1 g of bone). For the other concentrations, the excess of acid is much larger.

Each sample was withdrawn from the corresponding bath at pre-determined immersion times (6 h, 18 h, 24 h, 48 h and 72 h) and thoroughly washed in freezing water until neutral pH. These samples were again dried in vacuum oven at 40 °C until constant weight, to determine the respective final weight after demineralization.

2.3. Atomic Absorption Spectroscopy (AAS)

The calcium content of both the demineralized and the non-demineralized samples was determined by AAS, which required the previous removal of the bone organic matrix and subsequent dissolution of the mineral phase. For that purpose, each sample was calcined at 700 °C for 24 h and subsequently dissolved with concentrated HNO_3 at 80 °C. After dilution to a convenient concentration (1–5 ppm), the respective calcium concentration was determined using a PerkinElmer 3300 model (at 422.7 nm). The final result is the average of three independent measurements (each corresponding to 1/4 of slice) with 0.95 confidence level.

2.4. Thermal analysis

The control samples (natural cortical bone) were additionally submitted to Differential Scanning Calorimetry associated to Thermal Gravimetric Analysis (DSC-TGA) using the model Stanton Redford PL-STA 1500 from Polymer Laboratories. The obtained data enabled detailed information about the sample thermal decomposition and about the relative proportions of the bone matrix components (mineral, organic material and water). Samples were previously reduced to powder form (15–26 mg), by hand grinding in a ceramic mortar and pestle, and heated from 30 °C to 700 °C, at 10 °C/min, under oxidizing atmosphere using 55 ml/min flux of air.

2.5. XRD—X-Ray Diffraction Spectroscopy

XRD was used to monitor the phase composition features of the samples demineralized with 1.2 M HCl at various immersion times. The sample spectra were collected using a Phillips diffractometer operating in the Bragg–Brentano configuration with Co Kα ($\lambda = 1.78897$ Å) radiation at a current of 35 mA and an accelerating voltage of 40 kV. Spectra were recorded in the range $10° < 2\theta < 100°$ at a scanning speed of 7°/min and step size of 0.02°. The obtained X-ray patterns of the samples were compared with the pattern given by hydroxyapatite and assignments were based on the corresponding data from International Centre for Diffraction Data (ICDD; Powder Diffraction File no. 09-0432). The samples were partially reduced to powder form (~500 mg) before analysis.

2.6. FTIR—Fourier Transform Infrared Spectroscopy

FTIR was used to investigate alterations in the samples chemical composition caused by the demineralization process. Samples were reduced to powder form by scratching its surface (using about 10 mg per analysis). The resulting spectra were further compared with that from type I collagen, analysed using the same equipment. Occasionally, it was found necessary to examine the inner section of the samples in order to evaluate the progression of the demineralization reaction front. In these cases, the samples were fractured and the powder removed from its interior was subsequently analysed. The FTIR spectra were recorded in the range 400–4000 cm^{-1} in increments of 1.928 cm^{-1}, using the Magna FR-750 spectrometer from Nicolet in the attenuated total reflection (ATR) mode. Each spectrum was collected at room temperature at a nominal resolution of 4 cm^{-1} and the number of sample scans was 32.

2.7. Mercury porosimetry

Mercury porosimetry was used to measure the porosity and pore size distribution of the larger samples (half slices) demineralized for 24 h in different HCl solutions (0.6 M, 1.2 M and 2.4 M). Duplicate measurements were performed. A third sample was additionally used when the measured porosities differed by more than 5%. The reduced number of samples analysed by mercury intrusion (only those corresponding to 24 h) results from the relatively large quantity of sample needed for this technique (in comparison to the others used in this study) and, naturally, from the limited amount available. The porosimeter used was the Poresizer 9320 from Micromeritics and the pressure range varied between 0.5 psi and 30,000 psi, which enabled the measurement of pore diameters between 400 μm and 0.006 μm, respectively. Porosity was determined from the difference of the volumes of mercury intruded in the sample structure at these two extreme pressures. From the pressure *versus* intrusion data the equipment automatically generates cumulative and differential pore size distributions (based on the Washburn equation) (Lowell and Shields, 1991). Additionally, this technique enables the calculation of the bulk and skeletal densities, corresponding to the volumes measured at the lowest and the highest intrusion pressures, respectively. It should be stressed that the sample bulk volume includes almost all open pores whereas the skeletal density only includes pores smaller than the lower detection limit of the equipment (6 nm in the present case) (Lowell and Shields, 1991). The knowledge of these parameters is relevant, for instance, when the objective is to substitute one material by another with identical weight characteristics.

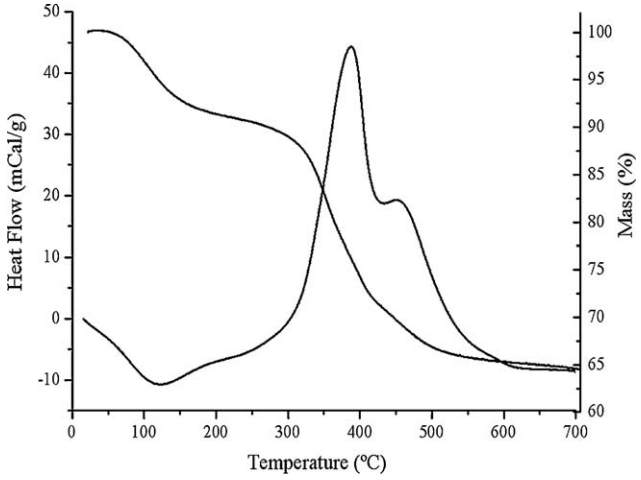

Fig. 1 – DSC-TGA profiles from non-demineralized bone samples, obtained under air atmosphere conditions.

2.8. Microscopy

Morphologic and microstructural analysis of the control and of the totally demineralized samples (70 h immersion in 1.2 M HCl) was performed using Light Microscopy and Scanning Electron Microscopy (SEM).

Light microscopy was performed using a Nikon Optiphot equipment. The surface lying in the plane perpendicular to the long axis of bone samples was polished using increasing grades of silicon carbide paper and finished with both 3 μm and 0.25 μm diamond suspension.

SEM observations were carried out in a Philips XL30 microscope operating at 5–15 kV. The test samples were mounted on a double-coated carbon conductive tape and copper sputter coated.

3. Results and discussion

3.1. Thermal analysis

DSC-TGA results of the non-demineralized sample, obtained under oxidizing conditions, between ambient temperature and 700 °C, are shown in Fig. 1.

The combined analysis of the thermogram (TGA curve) and the heat flow profile (DSC curve) indicates that the first weight loss (8%) occurs between 20 °C and 200 °C (peak at 108 °C) and corresponds to an endothermic process. The second weight

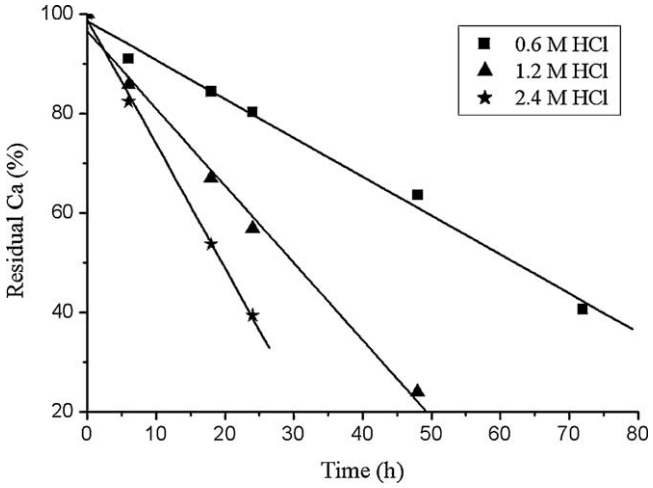

Fig. 2 – Residual calcium content (%) as a function of the immersion time (h) for different initial concentrations of HCl (0.6 M, 1.2 M and 2.4 M).

loss (27%) derives from exothermic reactions (peaks at 370 °C and 460 °C). These losses correspond, respectively, to the dehydration of the sample and to the decomposition of collagen and other residual organic components associated to this molecule (Lim, 1975; Peters et al., 2000; Mkukuma et al., 2004). These results show that the mineral content of bone is 65%. Considering that the mineral part of bone is essentially hydroxyapatite ($Ca_{10}(PO4)_6(OH)_2$), the calcium content of non-demineralized samples can then be estimated as 26% (0.40×0.65). However, it is frequently mentioned that bioapatites are usually calcium deficient due to the substitution of some ions in the crystal lattice (Lim, 1975; Peters et al., 2000; Mkukuma et al., 2004).

3.2. *Kinetics of demineralization*

As mentioned above, Atomic Absorption Spectroscopy (AAS) was used to assess the calcium content of the samples. In the case of the control sample (non-demineralized) the calcium content was determined as 26%, in excellent agreement with the value estimated from thermal analysis.

From the residual calcium content of the partially demineralized samples, at various immersion times and using distinct acid concentration, it was possible to determine the corresponding kinetic profiles. In these profiles, the non-demineralized samples were taken as reference, and thus their residual calcium content was taken as 100%.

The kinetic profiles representing the demineralization processes using initial concentrations of 0.6 M, 1.2 M and 2.4 M HCl (from 0 h to 72 h) are illustrated in Fig. 2 and can be described by a linear equation (Eq. (1)) of the type:

$$y = 100 - Kx \quad (1)$$

where y is the residual calcium percentage, x is the immersion time expressed in hours and K (the slope) is a constant. The values of K, representing the rate of demineralization, are listed in Table 1 together with the corresponding Coefficient of Determination (R^2).

As expected, the higher the acid concentration, the larger is the demineralization rate. Moreover, after 24 h immersion, the only sample that contains a residual calcium percentage less than 50% is the one treated with 2.4 M HCl. However, as Fig. 2 and Table 1 show, the decrease in the calcium content is more pronounced when the initial HCl concentration increases from 0.6 M to 1.2 M than when this concentration is increased from 1.2 M to 2.4 M (K value nearly doubled in the first situation whereas in the latter only an increase of 50% was observed). These findings are in agreement with the work of other authors that reported that the diffusion coefficient decreased significantly for higher acid concentration (>1 N) (Horneman et al., 2004). The explanation given was that higher proton concentration originates higher concentration of all the ions, resulting in higher friction forces between them, which in turn lower the increase of the demineralization rate. Other authors, however, attribute the reduction in diffusivity to the alteration of collagen and other bone matrix proteins, which progresses with immersion time and acid concentration (Lewandrowski et al., 1996).

Table 1 – K values of Eq. (1) and corresponding R^2.

[HCl] (mol/dm^3)	K (h^{-1})	R^2
0.6	0.811	0.9889
1.2	1.655	0.9847
2.4	2.558	0.9974

3.3. *XRD*

X-Ray Diffraction Spectroscopy was used to qualitatively evaluate the phase composition of bone samples throughout demineralization with 1.2 M HCl. The evolution of XRD patterns with demineralization time (0 h, 12 h, 24 h and 48 h) is illustrated in Fig. 3, together with the spectrum of hydroxyapatite.

The diffractogram of the control sample (0 h) presents some distinct diffraction peaks, attributed to the mineral phase, superimposed on a broad band indicating an amorphous phase that corresponds to the organic component of bone (type I collagen), as confirmed by FTIR in Section 3.4. The diffraction peaks, namely at $2\theta = 30.2°$, 37.1°, 46.6°, 54.8°, 58.2° and 62.7°, correspond to the most intense characteristic peaks

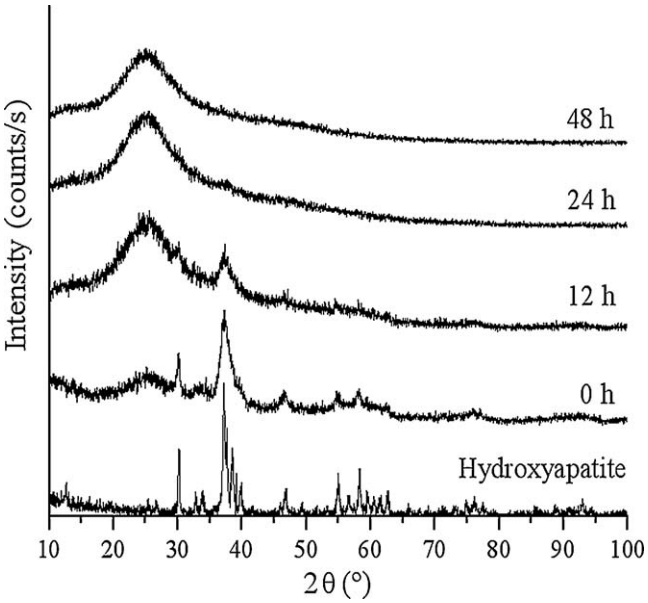

Fig. 3 – DRX of hydroxyapatite and of bone samples after different immersion times (0 h, 12 h, 24 h and 48 h) in 1.2 M HCl.

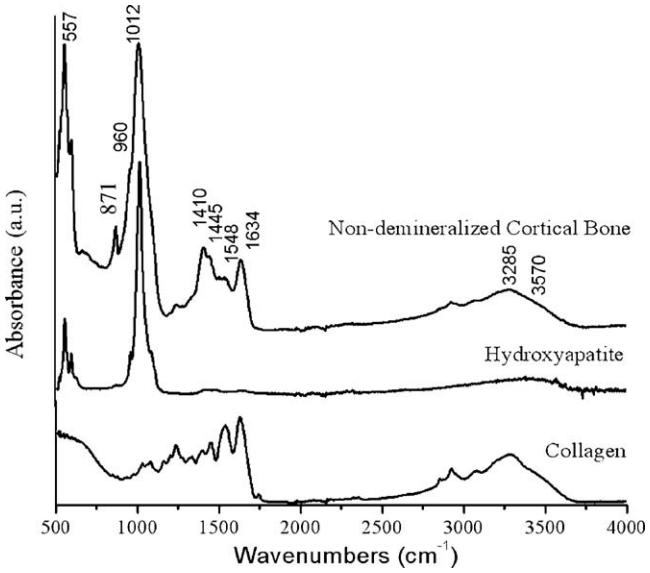

Fig. 4 – Comparison of the FTIR spectra of non-demineralized cortical bone, hydroxyapatite and collagen.

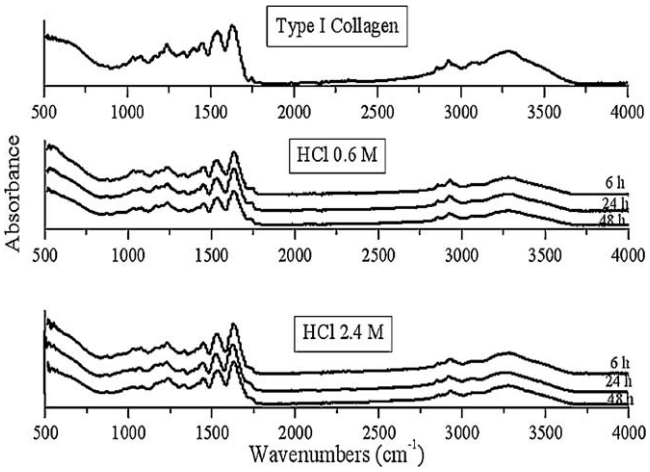

Fig. 5 – FTIR spectra of collagen and of bone samples after immersion in 0.6 M and 2.4 M HCl for 6 h, 24 h and 48 h.

of hydroxyapatite being respectively assigned to the following Miller plans: (0 0 2), (2 1 1), (3 1 0), (2 2 2), (1 2 3) and (0 0 4) (Danilchenko et al., 2002, 2004).

The evolution of XRD patterns with demineralization time is consistent with major phase differences detected in the analysed samples: from a poorly crystalline (t = 0 h) to completely amorphous (t = 48 h). After 12 h demineralization, only the most intense peaks from hydroxyapatite ((0 0 2) and (2 1 1)) could still be observed, whereas the others could not be clearly distinguished from the broad band of the amorphous phase. In addition to the decrease of the relative intensity of all diffraction lines (denoting the progressive decrease in the mineral content), a slight broadening of the (2 1 1) peak, in particular, was also observed. This is consistent with the decrease of the crystallinity of the hydroxyapatite, as well as of the crystal size (Danilchenko et al., 2004). At 24 h, the (2 1 1) peak was barely detectable and after 48 h, the diffractogram only revealed a broad band.

However, according to the kinetic data (Fig. 2), after 48 h immersion in 1.2 M HCl, the sample still contains 20% residual calcium relative to the control sample. This corresponds approximately to 5% calcium content (or 12.5% hydroxyapatite) in the sample total weight. Such low content may justify the non-detection of peaks from the mineral. In addition, the absence of the diffraction lines may also be due to the deterioration of the crystal lattice.

3.4. FTIR

FTIR was used to determine the chemical composition of bone samples before and after demineralization. The direct comparison of the spectra of the control sample with the spectra of hydroxyapatite and collagen (Fig. 4) confirm the dual-phase composition of natural bone. In fact, the most intense bands that occur at 557 cm^{-1} and 1012 cm^{-1} (with a shoulder at 961 cm^{-1}) are originated by phosphate stretching vibrations from the mineral component, whereas most bands above

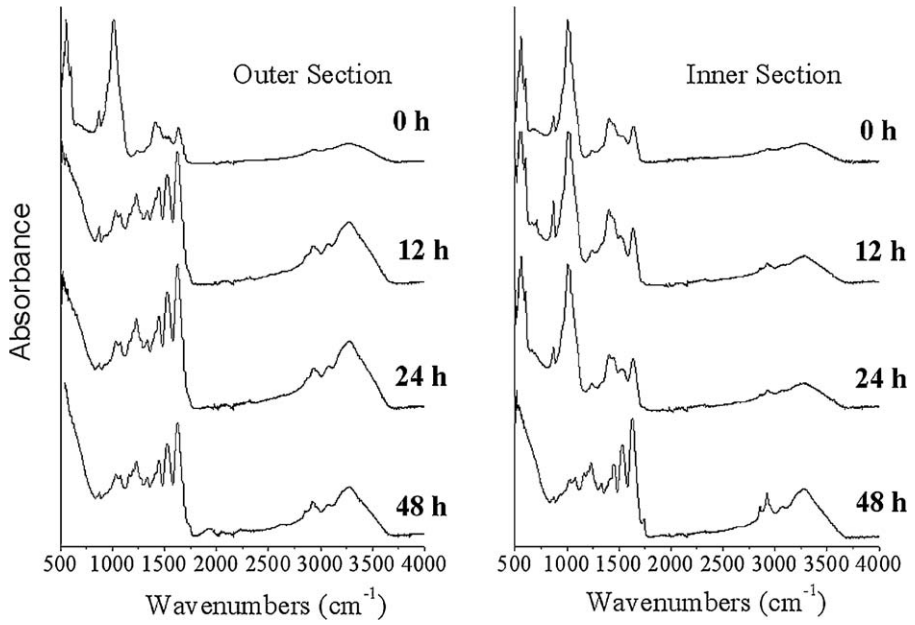

Fig. 6 – FTIR spectra from the outer (left) and inner (right) sections of the bone samples demineralized in 1.2 M HCl for different periods of time (0 h, 12 h, 24 h, 48 h, from top to bottom).

1500 cm^{-1} are assigned to vibrations from the amide groups from collagen (Mkukuma et al., 2004; Chang and Tanaka, 2002; Murugan et al., 2006). The peak around 3570 cm^{-1} corresponds to OH^- vibrations. Carbonate substitutions in the apatitic lattice of bone originate a peak at 871 cm^{-1} and a double band in the 1300–1450 cm^{-1} region (Rey et al., 1989).

The bone samples submitted to HCl demineralization under different experimental conditions were analysed by FTIR to monitor the consequent changes in their chemical composition. Fig. 5 shows the FTIR spectra of bone samples after demineralization with HCl for the two extreme acid concentrations (0.6 M and 2.4 M) and for periods of 6 h, 24 h and 48 h. The collagen spectrum was used for comparison. The absence of PO_4^{3-} bands and the similarity between these spectra and that from collagen suggests the complete demineralization of all samples for all the immersion times, independently of the acid concentration. This is definitely not compatible with the kinetic results. In fact, for immersion times up to 48 h in 0.6 M acid solution, samples still contain more than 50% residual calcium. The absence of the hydroxyapatite peaks, especially for the lower immersion times and/or lower acid concentrations, can, however, be explained by the fact that these spectra correspond to the powder that was removed from the outer surface of the samples. Since demineralization starts at the surface, the absence of the hydroxyapatite characteristics bands in the spectra of Fig. 5 was to be expected.

Moreover, these results suggest that an increase in acid concentration does not significantly affect the structure and composition of the collagen remaining in the demineralized samples.

In order to further examine the progression of the demineralization, a complementary study was performed with the samples decalcified in 1.2 M HCl. After immersion for 12 h, 24 h and 48 h, these samples were further fragmented to expose their interior. The fragments collected from their inner section were subsequently analysed by FTIR and compared with those of the outer section (Fig. 6). These results support the concept of a diffusion model and agree with the proposed theory of the unreacted core during demineralization (Horneman et al., 2004; Lewandrowski et al., 1996). In fact, the obtained spectra clearly show that, for the outer sections, the bands from hydroxyapatite are no longer detected after 12 h immersion, whereas for the inner sections, those bands only vanish after 48 h. Nonetheless, and as mentioned in the discussion of the XRD results, the latter samples still contain a small amount of calcium (<5%).

3.5. *Mercury porosimetry*

The main purpose of using mercury intrusion was to quantify the influence of the acid on the porosity/pore size distribution of the partially demineralized bone samples. The results obtained for 24 h immersion in 0.6 M, 1.2 M and 2.4 M HCl are illustrated in Fig. 7. In this figure, the cumulative intrusion curves of the samples tested are compared with the control sample (non-demineralized). As it can be seen, all curves present a similar profile, reflecting a significant intrusion of mercury in pore diameters between 300 μm and 10 μm (corresponding mostly to vascular porosity, that is, Harversian and Volkman Canals; Rho et al., 1998), followed by a range of no intrusion (plateau) and then another intrusion, although small, for pores smaller than 0.01 μm. The latter pores correspond to spaces between collagen fibres and apatite crystals (the so called collagen-apatite porosity; Rho et al., 1998; Cardoso et al., 2007).

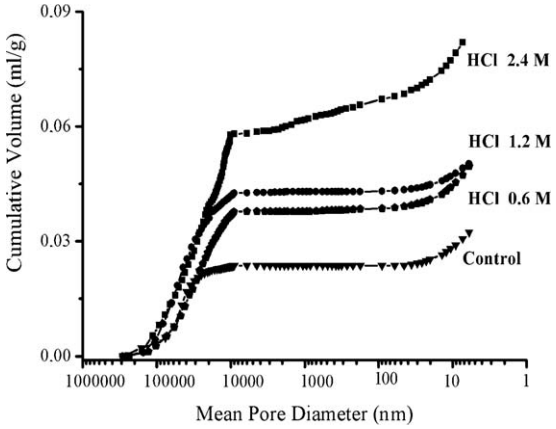

Fig. 7 – Cumulative mercury intrusion curves of the control sample and of the samples demineralized after 24 h immersion in 0.6 M, 1.2 M and 2.4 M HCl.

Nonetheless, the total intrusion volumes (related with porosity) present different values, depending upon the acid concentration (Table 2). As expected, the control sample corresponds to the lowest value of the intruded volume and the sample demineralized with 2.4 M HCl exhibits the highest value. In between are the curves corresponding to the samples immersed in 0.6 M and 1.2 M, which show little differences between them regarding mercury intrusion.

As mentioned before, intruded volume and porosity are not the only parameters measured by mercury porosimetry. Table 2 lists, in addition to mercury intruded volume, the values of bulk and skeletal density. The bulk density, defined as the ratio of the sample mass to the bulk volume, includes most sample pores. Similarly, the skeletal density corresponds to the skeletal volume, measured at the maximum intrusion pressure. For that, skeletal volume only includes the pores with apertures smaller than the lower limit of detection of the porosimeter used. Thus, the values measured for the bulk density are smaller than those of the skeletal density. The bulk density measured for the non-demineralized sample is in excellent agreement with the value reported for femoral cortical bone (1.85) (Karageorgiou and Kaplan, 2005).

In order to validate the measured skeletal densities, these were compared with the corresponding theoretical values based on the mineral and organic contents of the samples. These theoretical values (also reported on Table 2) were estimated considering the density of hydroxyapatite as 3.16 and that of the collagen and water as 1.0.

The analysis of these values leads to the following conclusions: (i) a significant increase was found for the porosity of the sample immersed in HCl 2.4 M (about 70%) relatively to the control sample (non-demineralized); (ii) for the lower acid concentrations, smaller and comparable increments were found (about 33% and 40%, respectively for HCl 0.6 M and 1.2 M); (iii) the same trend was observed for both the bulk and the skeletal densities; (iv) the skeletal densities are in excellent agreement with the theoretical values estimated from the sample composition; this proximity not only confirms the adequacy of the technique but also reveal that the amount of unmeasured pores (<3 nm) is not significant.

Table 2 – Results from mercury porosimetry (intruded volume, total porosity, bulk and skeletal density) for the bone samples demineralized for 24 h using 0.6 M, 1.2 M and 2.4 M HCl. Additionally, the values of the corresponding theoretical densities, estimated from the samples composition, are presented.

Parameter	Non-demineralized (control samples)	Demineralized samples in HCl		
		0.6 M	1.2 M	2.4 M
Intruded volume (cm^3/g)	0.032	0.049	0.050	0.085
Porosity (%)	6.20	8.25	8.70	10.60
Bulk density	1.89	1.72	1.66	1.25
Skeletal density	2.02	1.90	1.81	1.39
Theoretical density[a]	2.37	2.09	1.70	1.34

[a] Values estimated considering the density of hydroxyapatite as 3.16 and that of collagen and water both as 1.0. The composition of the control sample was taken as 65% hydroxyapatite and 35% water and collagen. The mineral contents of the partially demineralized samples were considered as 52%, 33% and 16%, respectively, for 0.6 M, 1.2 M and 2.4 M HCl. These values were calculated from the experimentally determined percentages of the samples residual calcium, considering the mineral part of these samples as hydroxyapatite.

3.6. *Microscopy*

Close examination of the fracture surfaces of the samples, before and after demineralization, was conducted to investigate the effects of the acid on the structural features of cortical bone (Figs. 8 and 9). As mentioned before, samples were visualized in a direction perpendicular to the long axis of the bone.

The images from the control samples (Fig. 8) clearly illustrate the basic structural unit of cortical bone (Haversian System), composed of concentric lamellae around a central canal (Haversian Canal). Numerous osteocyte lacunar spaces,

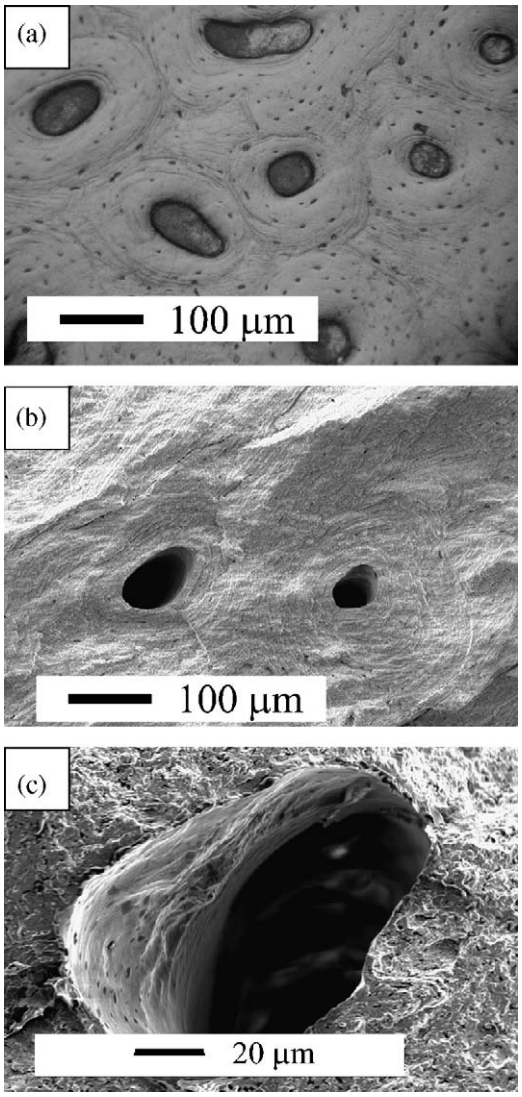

Fig. 8 – Light (a) and electron (b and c) photomicrographs of non-demineralized cortical bone matrix showing the microstructural organization of osteons composed of concentric lamellae around the Haversian Canal. Lacunar spaces and canaliculi are also visible.

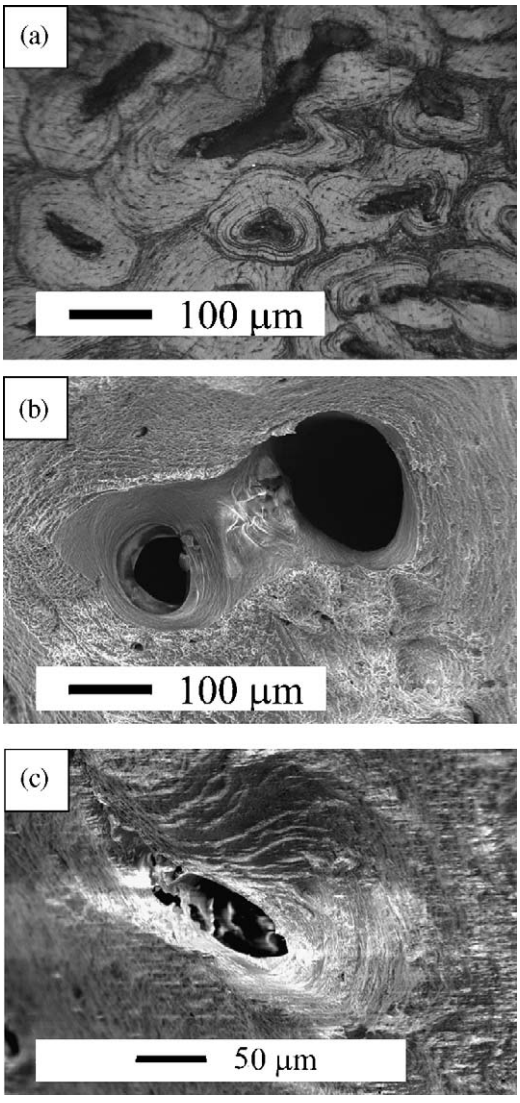

Fig. 9 – Light (a) and electron (b and c) images of demineralized bone samples (70 h in 1.2 M HCl). Most osteons present a structural deformation with irregular and increased diameter of the Haversian Canals.

entrapped in the lamellae and some canaliculi are also evident.

After the demineralization process, the basic microstructure of cortical bone matrix was preserved. Nevertheless, several morphological alterations were observed (Fig. 9). In fact, demineralized samples exhibited a certain degree of shrinkage, illustrated by a higher number of osteons per unit area (Fig. 9a). Structural deformation of most lamellae (Fig. 9a–c) and an increase in the diameter of the Haversian Canals was also evident (Fig. 9b). This is a consequence of the acidic removal of the apatite which causes the bone to lose most of its hardness and compressive resistance, leading to the deformation and collapse of the lamellae (Rho et al., 1998).

The preservation of the basic microstructure is consistent with the similar shape of the intrusion curves obtained from porosimetry for the control as well as for the demineralized samples (Fig. 7). Moreover, the increase in porosity measured by mercury intrusion for the demineralized samples (Table 2) is correlated to the increase in the diameter of the canals observed for these samples by microscopy.

4. Conclusions

The above results clearly show the modifications caused by the different demineralization procedures with respect to acid concentration. The first, and expected, conclusion was that the higher the initial acid concentration the higher the demineralization rate. Nonetheless, from the linear kinetic profiles, it could be concluded that this rate is not directly proportional to the HCl concentration: a relatively larger increment was observed when HCl was increased from 0.6 M to 1.2 M than that found when the concentration was varied from 1.2 M to 2.4 M.

XRD spectra have shown the evolution of bone phase composition with the immersion time, from a low crystalline material with a dual-phase composition to a completely amorphous structure. The gradual decrease in the intensity of the hydroxyapatite peaks and the broadening of their width are consistent with the removal of the mineral from the bone matrix and with the crystal lattice degradation. However, it should be pointed out that the absence of the typical hydroxyapatite peaks does not necessarily indicate the total demineralization of the bone samples.

Since FTIR provided information about local chemical composition of the bone samples (internal and external surfaces), it was possible to confirm the diffusional character of the demineralization process. Despite all the FTIR spectra of the partially demineralized samples surface being similar and identical to that of the pure collagen, it would be interesting to investigate whether the collagen fibrils of the sample subjected to the highest acid concentrations were, to any extent, deteriorate. FTIR did not seem to be sensitive enough to elucidate this point, neither to detect hydroxyapatite peaks in low calcium contents samples.

As for the structural modifications, mercury intrusion revealed that the highest acid concentration resulted in the highest sample porosity and, consequently, in the lowest values of bulk and skeletal densities. Curiously the samples immersed in 0.6 and 1.2 M HCl exhibited very similar structural features.

Microscopic observations not only confirmed the existence of pores in the range of the mercury intrusion curves for the control and demineralized samples, but also illustrated the preservation of the basic structure of bone after demineralization, in spite of significant morphological alterations.

References

Bae, H.W., Zhao, L., Kanim, L.E.A., Wong, P., Delamarter, R.B. and Dawson, E.G., 2006, Intervariability and intravariability of bone morphogenetic proteins in commercially available demineralized bone matrix products. Spine, 31(12): 1299–1306.

Bauer, T.W. and Muschler, G.F., 2000, Bone graft materials. An overview of the basic science. Clin Orthop Relat Res, 371: 10–27.

Cardoso, A.V., Oliveira, W.J. and Vaz, G.J.O., 2007, Cortical bone porosity visualization using mercury porosimetry intrusion data. Revista Matéria, 12(4): 612–617.

Chang, M.C. and Tanaka, J., 2002, FT-IR study for hydroxyapatite/collagen nanocomposite cross-linked by glutaraldehyde. Biomaterials, 23(24): 4811–4818.

Colnot, C., Romero, D.M. and Huang, S., 2005, Mechanism of action of demineralized bone matrix in the repair of cortical bone defects. Clin Orthop Relat Res, 435: 69–78.

Costa, A., Oliveira, C., Leopizzi, N. and Amatuzzi, M., 2001, The use of demineralized bone matrix in the repair of osteochondral lesions. Experimental study in rabbits. Acta Ortop Bras, 9(4): 27–38.

Danilchenko, S.N., Kukharenko, O.G., Moseke, C., Protsenko, L.Y., Sukhodub, L.F. and Sulkio-Cleff, B., 2002, Determination of the bone mineral crystallite size and lattice strain from diffraction line broadening. Cryst Res Technol, 37(11): 1234–1240.

Danilchenko, S.N., Moseke, C., Sukhodub, L.F. and Sulkio-Cleff, B., 2004, X-ray diffraction studies for bone apatite under acid demineralization. Cryst Res Technol, 39(1): 71–77.

Dorozhkin, S.V., 1997, Surface reactions of apatite dissolution. J Colloid Interface Sci, 191(2): 489–497.

Eppley, B.L., Pietrzak, W.S. and Blanton, M.W., 2005, Allograft and alloplastic bone substitutes: a review of science and technology for the craniomaxillofacial surgeon. J Craniofac Surg, 16(6): 981–989.

Hansen, H.B., 1974, Kinetics of acid demineralization in histological technique. J Histochem Cytochem, 22(6): 434–441.

Horneman, D.A., Ottens, M., Hoorneman, M. and Van der Wielen, L.A.M., 2004, Reaction and diffusion during demineralization of animal bone. AIChE J, 50(11): 2682–2690.

Judas, F., Teixeira, L. and Proença, A., 2005, Coimbra University Hospitals' Bone and Tissue Bank: twenty-two years of experience. Transplant Proc, 37: 2799–2801.

Karageorgiou, V. and Kaplan, D., 2005, Porosity of 3D biomaterial scaffolds and osteogenesis. Biomaterials, 26: 5474–5491.

Katz, M., Nataraj, C., Jaw, R., Deigl, E. and Bursac, P., 2008, Demineralized bone matrix as an osteoinductive biomaterial and in vitro predictors of its biological potential. J Biomed Mater Res B, 89B(1): 127–134.

Kim, S.G., Kim, W.K., Park, J.C. and Kim, H.J., 2002, A comparative study of osseointegration of Avana implants in a demineralized freezedried bone alone or with platelet-rich plasma. J Oral Maxillofac Surg, 60: 1018–1025.

Kucukkolbasi, H., Mutlu, N., Isik, K., Celik, I. and Oznurlu, Y., 2009, Histological evaluation of the effects of bioglass, hydroxyapatite, or demineralized freeze-dried bone, grafted alone or as composites, on the healing of tibial defects in rabbits. Saudi Med J, 30(3): 329–333.

Lee, Y.P., Jo, M., Luna, M., Chien, B., Lieberman, J.R. and Wang, J.C., 2005, The efficacy of different commercially available demineralized bone matrix substances in an athymic rat model. J Spinal Disord Tech, 18(October (5)): 439–444.

Lewandrowski, K.U., Tomford, W.W., Michaud, N.A., Schomacker, K.T. and Deutsch, T.F., 1997, An electron microscopic study on the process of acid demineralization of cortical bone. Calcif Tissue Int, 61: 294–297.

Lewandrowski, K.U., Venugopalan, V., Tomford, W.W., Schomacker, K.T., Mankin, H.J. and Deutsch, T.F., 1996, Kinetics of cortical bone demineralization: controlled

demineralization—a new method for modifying cortical bone allografts. J Biomed Mater Res, 11(3): 365–372.
Libin, B.M., Ward, H.L. and Fishman, L., 1975, Decalcified, lyophilized bone allografts for use in human periodontal defects. J Periodontol, 46: 51–56.
Lim, J.J., 1975, Thermogravimetric analysis of human femur. J Biol Phys, 30(3): 111–129.
Lohmann, C.H., Andreacchio, D., Köster, G., Carnes, D.L., Jr., Cochran, D.L., Dean, D.D., Boyan, B.D. and Schwartz, Z., 2001, Tissue response and osteoinduction of human bone grafts in vivo. Arch Orthop Trauma Surg, 121: 583–590.
Lomas, R.J., Gillan, H.L., Matthews, J.B., Ingham, E. and Kearney, J.N., 2001, An evaluation of the capacity of differently prepared demineralized bone matrices (DBM) and toxic residuals of ethylene oxide (EtOx) to provoke an inflammatory response in vitro. Biomaterials, 22: 913–921.
Lowell, S. and Shields, J.E., (1991). *Powder Surface Area and Porosity* (3rd ed.). (Chapman and Hall, London).
Martin, G.J., Jr, Boden, S.D., Titus, L. and Scarborough, N.L., 1999, New formulations of demineralized bone matrix as a more effective graft alternative in experimental posterolateral lumbar spine arthrodesis. Spine, 24: 637–645.
Mkukuma, L.D., Skakle, J.M.S., Gibson, I.R., Imrie, C.T., Aspden, R.M. and Hukins, D.W.L., 2004, Effect of the proportion of organic material in bone on thermal decomposition of bone mineral: an investigation of a variety of bones from different species using thermogravimetric analysis coupled to mass spectrometry, high temperature X-ray diffraction and Fourier transform infrared spectroscopy. Calcif Tissue Int, 75(4): 321–328.
Morone, M.A. and Boden, S.D., 1998, Experimental posterolateral lumbar spinal fusion with a demineralized bone matrix gel. Spine, 23: 159–167.
Murugan, R. and Ramakrishna, S., 2004, Modification of demineralized bone matrix by a chemical route. J Mater Chem, 14: 2041–2045.
Murugan, R., Ramakrishna, S. and Rao, K.P., 2006, Nanoporous hydroxyl-carbonate apatite scaffold made of natural bone. Mater Lett, 60(3): 2844–2847.
Nade, S. and Burwell, R.G., 1977, Decalcified bone as a substrate for osteogenesis: an appraisal of the interrelation of bone and marrow in combined grafts. J Bone Joint Surg, 59-B(2): 189–196.
Peters, F., Schwarz, K. and Epple, M., 2000, The structure of bone studied with synchrotron X-ray diffraction, X-ray absorption spectroscopy and thermal analysis. Thermochim Acta, 361: 131–138.
Peterson, B., Whang, P.G., Iglesias, R., Wang, J.C. and Lieberman, R.J., 2004, Osteoinductivity of commercially available demineralized bone matrix. Preparations in a spine fusion model. J Bone Joint Surg, 86: 2243–2250.
Pietrzak, W.S., Ali, S.N., Chitturi, D., Jacob, M. and Woodell-May, J.E., 2009, BMP depletion occurs during prolonged acid demineralization of bone: characterization and implications for graft preparation. Cell Tissue Bank, doi:10.1007/s10561-009-9168-6.
Pietrzak, W., Perns, S.V., Keyes, J., Woodell-May, J. and McDonald, N., 2005, Demineralized bone matrix graft: a scientific and clinical case study assessment. J Foot Ankle Surg, 44: 345–353.
Rey, C., Collins, B., Goehl, T., Dickson, I.R. and Glimcher, J., 1989, The carbonate environment in bone mineral: a resolution-enhanced Fourier transform infrared spectroscopy study. Calcif Tissue Int, 25(3): 157–164.
Rho, J., Spearing, L. and Zioupos, P., 1998, Mechanical properties and the hierarchical structure of bone. Med Eng Phys, 120: 92–102.
Schwartz, Z., Mellonig, J.T., Carnes, D.L., Jr, de la Fontaine, J., Cochran, D.L., Dean, D.D. and Boyan, B.D., 1996, Ability of commercial demineralized freeze-dried bone allograft to induce new bone formation. J Periodontol, 67: 918–926.
Traianedes, K., Russell, J.L., Edwards, J.T., Stubbs, H.A., Shanahan, I.R. and Knaack, D., 2004, Donor age and gender effect on osteoinductivity of demineralized bone matrix. J Biomed Mater Res B, 70(1): 21–29.
Tuli, S.M. and Singh, A.D., 1978, The osteoinductive property of decalcified bone matrix. J Bone Joint Surg, 60-B(1): 116–123.
Urist, M.R., 1965, Bone formation by autoinduction. Science, 150: 893–899.
Zhang, M., Powers, R.M., Jr. and Wolfinbarger, L., Jr., 1997, Effect(s) of the demineralization process on the osteoinductivity of demineralized bone matrix. J Periodontol, 68: 1085–1092.
Walsh, W.R. and Christiansen, D.L., 1995, Demineralized bone matrix as a template for mineral-organic composites. Biomaterials, 16: 1363–1371.